Decision on submission to Sustainable Energy Technologies and Assessments

em.seta.0.731e0f.c514c819@editorialmanager.com
<em.seta.0.731e0f.c514c819@editorialmanager.com>
on behalf of
Sustainable Energy Technologies and Assessments <em@editorialmanager.com>
Thu 06/05/2021 17:25

To: Muhumuza, Ronald <r.muhumuza@ulster.ac.uk>

[You don't often get email from em@editorialmanager.com. Learn why this is important at http://aka.ms/LearnAboutSenderIdentification.]

[EXTERNAL EMAIL]

CC: meng.ni@polyu.edu.hk

Manuscript Number: SETA-D-21-00028R1

Meeting energy needs of low-income sub Saharan households with a Partially Hybridised Solar Technology (PHST): Experimental performance evaluation based on simulated solar radiation and demand profiles

Dear Dr. Muhumuza,

Thank you for submitting your manuscript to Sustainable Energy Technologies and Assessments.

I am pleased to inform you that your manuscript has been accepted for publication.

My comments, and any reviewer comments, are below.
Your accepted manuscript will now be transferred to our production department. We will create a proof which you will be asked to check, and you will also be asked to complete a number of online forms required for publication. If we need additional information from you during the production process, we will contact you directly.

We appreciate you submitting your manuscript to Sustainable Energy Technologies and Assessments and hope you will consider us again for future submissions.

Kind regards,
Prof. Meng Ni, The Hong Kong Polytechnic University
Senior Editor, Sustainable Energy Technologies and Assessments
meng.ni@polyu.edu.hk
https://eur03.safelinks.protection.outlook.com/?url=https%3A%2F%2Fpublons.com%2Fresearcher%2F1368068%2Fmeng-ni%2F&data=04%7C01%7Cr.muhumuza%40ulster.ac.uk%7C20fb8c8340014f2c816208d910ab85c6%7C6f0b94874fa842a8aeb4bf2e2c22d4e8%7C0%7C0%7C637559151135456945%7CUnknown%7CTWFpbGZsb3d8eyJWIjoiMC4wLjAwMDAiLCJQIjoiV2luMzIiLCJBTiI6Ik1haWwiLCJXVCI6Mn0%3D%7C1000&sdata=Ds16Y12Mor%2Blwb7cFh%2FjS%2FI2EY4Bw6S7PpHLUTSJLto%3D&reserved=0

Editor and Reviewer comments:

Reviewer #3: The authors addressed all this reviewer comments

More information and support

FAQ: When and how will I receive the proofs of my article?
https://eur03.safelinks.protection.outlook.com/?url=https%3A%2F%2Fservice.elsevier.com%2Fapp%2Fanswers%2Fdetail%2Fa_id%2F6007%2Fp%2F10592%2Fsupporthub%2Fpublishing%2Frelated%2F&data=04%7C01%7Cr.muhumuza%40ulster.ac.uk%7C20fb8c8340014f2c816208d910ab85c6%7C6f0b94874fa842a8aeb4bf2e2c22d4e8%7C0%7C0%7C637559151135456945%7CUnknown%7CTWFpbGZsb3d8eyJWIjoiMC4wLjAwMDAiLCJQIjoiV2luMzIiLCJBTiI6Ik1haWwiLCJXVCI6Mn0%3D%7C1000&sdata=f0ajODjZNjTJVwrlrAYKnEl81ewuyaqO2hN6JQ2nh4M%3D&reserved=0

You will find information relevant for you as an author on Elsevier's Author Hub:
https://eur03.safelinks.protection.outlook.com/?url=https%3A%2F%2Fwww.elsevier.com%2Fauthors&data=04%7C01%7Cr.muhumuza%40ulster.ac.uk%7C20fb8c8340014f2c816208d910ab85c6%7C6f0b94874fa842a8aeb4bf2e2c22d4e8%7C0%7C0%7C637559151135456945%7CUnknown%7CTWFpbGZsb3d8eyJWIjoiMC4wLjAwMDAiLCJQIjoiV2luMzIiLCJBTiI6Ik1haWwiLCJXVCI6Mn0%3D%7C1000&sdata=FD6AvlQbmF3OFsmJC3utIQHd9y9NGxltct%2Fwp2B7hRU%3D&reserved=0

FAQ: How can I reset a forgotten password?
https://eur03.safelinks.protection.outlook.com/?url=https%3A%2F%2Fservice.elsevier.com%2Fapp%2Fanswers%2Fdetail%2Fa_id%2F28452%2Fsupporthub%2Fpublishing%2F&data=04%7C01%7Cr.muhumuza%40ulster.ac.uk%7C20fb8c8340014f2c816208d910ab85c6%7C6f0b94874fa842a8aeb4bf2e2c22d4e8%7C0%7C0%7C637559151135456945%7CUnknown%7CTWFpbGZsb3d8eyJWIjoiMC4wLjAwMDAiLCJQIjoiV2luMzIiLCJBTiI6Ik1haWwiLCJXVCI6Mn0%3D%7C1000&sdata=ttv%2BZa0z1Tph1gZmkpltVkLcOhdObYMJrZIfdd8rlO4%3D&reserved=0
For further assistance, please visit our customer service site:
https://eur03.safelinks.protection.outlook.com/?url=https%3A%2F%2Fservice.elsevier.com%2Fapp%2Fhome%2Fsupporthub%2Fpublishing%2F&data=04%7C01%7Cr.muhumuza%40ulster.ac.uk%7C20fb8c8340014f2c816208d910ab85c6%7C6f0b94874fa842a8aeb4bf2e2c22d4e8%7C0%7C0%7C637559151135456945%7CUnknown%7CTWFpbGZsb3d8eyJWIjoiMC4wLjAwMDAiLCJQIjoiV2luMzIiLCJBTiI6Ik1haWwiLCJXVCI6Mn0%3D%7C1000&sdata=8%2FI7deU0Z8%2BTMjl2kgYRpGU6z7f%2BV8%2Fv2k8XDLdupfQ%3D&reserved=0
Here you can search for solutions on a range of topics, find answers to frequently asked questions, and learn more about Editorial Manager via interactive tutorials. You can also talk 24/7 to our customer support team by phone and 24/7 by live chat and email

---

data=04%7C01%7Cr.muhumuza%40ulster.ac.uk%7C20fb8c8340014f2c816208d910ab85c6%7C6f0b94874fa842a8aeb4bf2e2c22d4e8%7C0%7C0%7C637559151135466939%7CUnknown%7CTWFpbGZsb3d8eyJWIjoiMC4wLjAwMDAiLCJQIjoiV2luMzIiLCJBTiI6Ik1haWwiLCJXVCI6Mn0%3D%7C1000&sdata=1d7cqW46FuGV5NBmTYjgngXgXw032Kp85R4k3ltac3U%3D&reserved=0). Please contact the publication office if you have any questions.

Meeting energy needs of low-income Sub-Saharan households with a Partially Hybridised Solar Technology (PHST): Experimental performance evaluation based on simulated solar radiation and demand profiles

Ronald Muhumuza[1,a,b], Aggelos Zacharopoulos[a], Jayanta Deb Mondol[a], Mervyn Smyth[a,c], Adrian Pugsley[a]

[a] Centre for Sustainable Technologies, Belfast School of Architecture and the Built Environment, Ulster University, Newtownabbey, BT37 0QB, Northern Ireland, UK

[b] Faculty of Engineering, Department of Agro-processing Engineering, Busitema University, P.O. Box 236, Tororo, Uganda

[c] SolaForm Ltd (www.solaform.com) c/o Ulster University, Newtownabbey, BT37 0QB, Northern Ireland, UK

Abstract

Renewable energy technologies for sustainable development are rapidly attracting attention across many disciplines despite technical, economic, and social barriers that limit application beyond the laboratory. This study proposes novel semi-automated and automated domestic hot water and electricity demand simulation experiments to evaluate the performance of a proof-of-concept prototype under simulated solar conditions. The prototype is a Partially Hybridised Solar Technology (PHST) which integrates photovoltaic (PV) and low-temperature solar thermal technology for low-cost electricity and domestic hot water supply. The domestic hot water and electrical demand profiles, and the solar radiation utilised during the study represent typical conditions of off-grid households in Sub-Saharan Africa. The prototype delivered a thermal energy supply potential of $2{,}073 \pm 75$ kJ per day at an average solar thermal conversion efficiency of $29.4 \pm 1.0\%$. The average yield of Direct Current (DC) electricity was 273 Wh per day at a corresponding PV module efficiency of 12.1% but depended on the type of charge controller. These results provide essential baselines for future computer modelling work and techno-economic predictions for Sub-Saharan Africa. The study has important future implications to test standards guiding laboratory-based evaluation of Solar Home Systems (SHSs) for electricity and domestic hot water.

[1] Corresponding author.
E-mail address: r.muhumuza@ulster.ac.uk (R. Muhumuza), a.zacharopoulos@ulster.ac.uk (A. Zacharopoulos), jd.mondol@ulster.ac.uk (J. Deb Mondol), m.smyth1@ ulster.ac.uk

Keywords: Experimental simulation; solar thermal; ICSSWH; solar PV; cogeneration; off-grid energy access

Nomenclature

PRV	Pressure-reducing valve
MPPT	Maximum Power Point Tracking
PWM	Pulse-width modulation
AFRICaS	Asymmetric Formed Reflector with Integrated Collector and Storage
PHST	Partially Hybridised Solar Technology
PV/T	Photovoltaic-Thermal
ICSSWH	Integrated Collector Storage Solar Water Heater
CVMI	Current-Voltage Measurement Interface
LED	Light Emitting Diode
A_{PV}	PV cell surface area (m^2)
A_P	AFRICaS ICSSWH subsystem aperture area (m^2)
m_w	Water mass delivered during each draw-off (kg)
$C_{p,w}$	specific heat capacity of water at constant pressure (J/kg K)
v_t	Water storage tank volume of the ICSSWH (m^3)
F_{Dm}	Diffuse fraction of horizontal radiation (-)
G_{min}	Minimum intensity measured across the PV module aperture (W/m^2)
G_{avg}	Average intensity measured across the AFRICaS ICSSWH aperture (W/m^2)
$H(\beta = 0°)$	Monthly average daily Global Horizontal Irradiation ($kWh/m^2/day$)
$H_T(\beta = 15°)$	Monthly average daily irradiation at a surface tilt angle of 15° ($kWh/m^2/day$)
I_{PV}	Current supplied by the PV module (A)
I_m	Current supplied by the PV module at Maximum Power Point (A)
I_{SC}	Short circuit current of PV module (A)
K_{Tm}	Clearness index (-)
V_m	PV module voltage at Maximum Power Point (V)
P_m	PV module power at Maximum Power Point (W)
V_{PV}	Voltage generated by the PV module (V)
E_{PV}	Energy yield from the PV module (Wh)
E_L	Energy supplied to the load (Wh)
$E_{Sim \to ICS}$	Energy supplied by solar simulator onto the AFRICaS ICSSWH aperture (J)
$E_{Sim \to PV}$	Energy supplied by solar simulator onto the PV module aperture (W)
Q_{HW_j}	Thermal energy delivered calculated for a draw-off volume j (J)

63	Q_L	Electric charge equivalent of energy supplied to the load (Ah)
64	T	Temperature (°C)
65	ρ	water density ($\mathrm{kg/m^3}$)
66	Δt	The period of simulated solar irradiance (s)
67	j	the j^{th} hot water draw-off count, 1,2,…N
68	β	Surface tilt angle (°)
69	η	Efficiency (%)

1. Introduction

Hybridisation of photovoltaic (PV) technologies and solar thermal technologies for generating electricity and domestic hot water is an essential concept in enabling affordable and safe access to modern energy. Recent research on this topic is generating significant knowledge and interest in developing countries under the frame of Sustainable Development Goal (SDG) #7 [1]. These technologies, which are conceived as flatpack or modular concepts are fundamental for increasing the solar energy yield per unit area to enhance economic feasibility and optimise available land. Furthermore, modularising certain readily available and/or market ready solar technologies enhances flexibility, scaleability and rapid deployement times to achieve low cost designs [2]. These considerations can result in Partially Hybridised Solar Technology (PHST) as an alternative concept, i.e., a form of Solar Energy Cogeneration (SEC) [3] which differs from Photovoltaic-Thermal (PV/T) technology [4–8] due to the reasons explained next.

A standard PV module is readily available at a low price whereas PV/T units are specialist products which are more expensive and much less readily available. There may be an efficiency and temperature advantage to having the PV and thermal separate. In cases where electricity is the dominant demand, the temperature of a PV/T collector is usually limited so that the electrical efficiency can be maximised (typically 0.45%/°C [9] reduction in electrical output for crystalline silicon PV). In cases where heat needs to be produced at a high temperature (e.g., domestic hot water at >60°C) the electrical efficiency will inherently be compromised by the temperature effect. In addition, high temperatures usually require a transparent cover, which also reduces optical efficiency. Covered PV/T collectors can easily suffer stagnation damage when there is no demand for heat or if heat extraction pumps/fans/systems fail. This is a problem in the developing country context where access to parts and maintenance expertise might be limited and water supplies might be unreliable. Having the PV separate from the thermal protects it from stagnation damage.

The PHST concept significantly relaxes or eliminates the fundamental aspect of managing the PV cell operating temperature for improving the efficiency of electricity generation in PV/T technologies. This minimises complexity in modular PHST units and eases maintenance requirements, which is of significant necessity owing to technical capability limitations [10] in remote off-grid locations of developing countries. A variety of other potential systems including Low Concentration Photovoltaic (LCPV) systems [11], concentrating photovoltaic-thermal (CPV/T) systems [12,13] and Concentrated Solar Power (CSP) systems [14] could be considered but they present a lack of field operational experience in remote off-grid areas or are large scale and capital intensive.

To advance with PHST concepts, it is essential to determine the minimum practicable energy demand to be satisfied at the scale of a single module. The multi-tier energy access and technology design framework [15] of the World Bank and the matrix of quantified energy use estimates proposed by Muhumuza et al. [16] can be helpful. For example, Table 1 shows an electrical demand scenario of up to 250 Wh per day which provides electricity supply to enable essential basic energy services for remote households at tier 2 level [17,18]. This daily demand is similar to that of Ayeng'o et al. [19] measured for an off-grid Solar Home System (SHS) in Tanzania. A typical off-grid households in developing countries could have an average domestic hot water demand of 5.6 L per person per day [20,21], i.e., 28 L per day for a 4-person household. By contrast, a low hot water demand situation for households in developed countries would be 30 L per person per day or 120L/day for a 4-person household [22–25]. To raise the temperature by 20°C of 28 L water from a mean temperature of say 25°C for domestic purposes could demand 1,408 kg of traditional fuelwood per household per year as estimated in Table 2. The reality of these coexisting energy demands and the potential for cost effective solar solutions represents an interesting technology research and development dimension.

Table 1
Estimated energy demand for an entry-level PV component at tier 2 level as a subsystem of the proposed PHST.

Appliances/ Loads	**Power rating (watts)**	**Daily Hours of use (hrs)**	**No of appliances**	**Watt-hours per day (Wh/day)**
LED indoor	5	4	3	60
LED security	5	8	2	80
Phone charger	5	2	1	10
Fan	15	4	1	60
Radio	10	4	1	40
			Energy needed	**250**

Table 2
Quantity of primary fuelwood estimate (kg per household per year) to produce a temperature rise of 20 °C for 28 L/day of low temperature hot water [26].

Detail	**Value**	**Unit**
Initial temperature	25	°C
Final temperature	45	°C
Estimated demand for low temperature hot water	28	L/day
Useful energy required for water heating from 25°C to 45°C	2.34	MJ/day
Heat loss coefficient (assumed typical for a water heating appliance)	4	W/K
Thermal energy losses over the day (24 hour)	7	MJ/day
Gross energy requirement	9.26	MJ/day
Overall efficiency of the water heating appliance, assuming traditional fuelwood cook stove [27]	15	%
Primary thermal energy requirement	61.71	MJ/day
Annual primary thermal energy requirement	22,523.32	MJ/year
Typical thermal energy content of fuelwood	16	MJ/kg
Mass of fuelwood required	1,407.71	kg/year

PHSTs are a decoupled combination of readily available individual solar thermal and PV subsystems. They can combine subsystems of clean and conventional technologies in a less complex and modular fashion. The range of technology combinations is unlimited and can comprise subsystems along with conventional devices such as DC resistance heating, energy storage, optical elements (reflectors or concentrators), net metering, smart controls, etc. To service multiple households within a close distance range, the PV subsystems of the various PHST units could interconnect in a DC nano-grid (also known as a micro-grid or a mini-grid [28]) and the solar thermal subsystems in a small-scale district heating system. A parallel connection of the PV subsystems in a DC nano-grid produces a stable voltage supply. Solar thermal subsystems connected in parallel achieve redundancy whilst series thermal systems may deliver thermal energy with a higher temperature rise. Additionally, cost effective/affordable PHSTs may be achieved through the removal, substantial reduction, or substitution of certain auxiliary components, e.g., pumps, pipework and controls.

If readily available, Integrated Collector Storage Solar Water Heater (ICSSWH) technologies [29,30] can be attractive in formulating PHSTs. They combine the solar thermal energy collection and storage functions into a single unit with no moving parts, allowing users to be independent of grid electricity [31]. While they are affordable and less complex for domestic hot water, they may require alternative structures and materials to improve their thermal energy collection and retention efficiencies. Pugsley et al. [32,33] have created flexible and rapidly deployable PHST prototypes for field testing at a remote off-grid location in Botswana. Each prototype incorporated a flat reflector, a thermal diode ICSSWH [34] and a standard polycrystalline PV module. Many commercial and pre-commercial ICSSWHs are arguably featured in literature as low-cost technology for low temperature domestic water heating. Various studies in Dominican Republic [35], Greece [36,37], Tunisia [38], Egypt [39] and India [40] among others have demonstrated the potential success of various ICSSWH concepts that fit well the scope of readily available solar thermal technologies. Recent research is developing modelling approaches [41] and introducing modifications in individual componentry [34,42] to facilitate commercialisation and the development of cost-effective PHSTs. Technology affordability for modern energy access is a critical aspect of Willingness To Pay (WTP) which is a measure of the potential technology uptake based on the financial buying ability of users and the resulting long-term satisfaction derived from the purchased technology [43].

Muhumuza et al. [44,45] aimed for a packaged PHST or flatpack design referred to as the Asymmetric Formed Reflector with Integrated Collector and Storage (AFRICaS) system. The system integrated PV technology and introduced a non-imaging Compound Parabolic Concentrator (CPC) for improved solar thermal collection performance of the cylindrical thermal diode ICSSWH. The reported optical performance results [45] of the AFRICaS ICSSWH subsystem indicated potential success for water heating at equatorial latitudes. Fig. 1 depicts the overall definition of the modular AFRICaS PHST proposition to support combined basic electricity and thermal energy demands at an entry-level scale for off-grid households in developing countries.

This paper develops an experimental testing methodology to evaluate the performance of a single AFRICaS PHST prototype under simulated conditions. The testing program employs experimentally simulated Direct Current (DC) electrical energy demand profiles and hot water draw-off patterns derived from realistic field measurements and published literature. Firstly, the paper addresses technical sizing of components and presents the experimental simulations methodology in section 2 and section 3, respectively. Then in section 4, the paper reports and discusses the results of lab-based technical findings for the hot water and electricity subsystems of the AFRICaS PHST prototype and the conclusion in section 5.

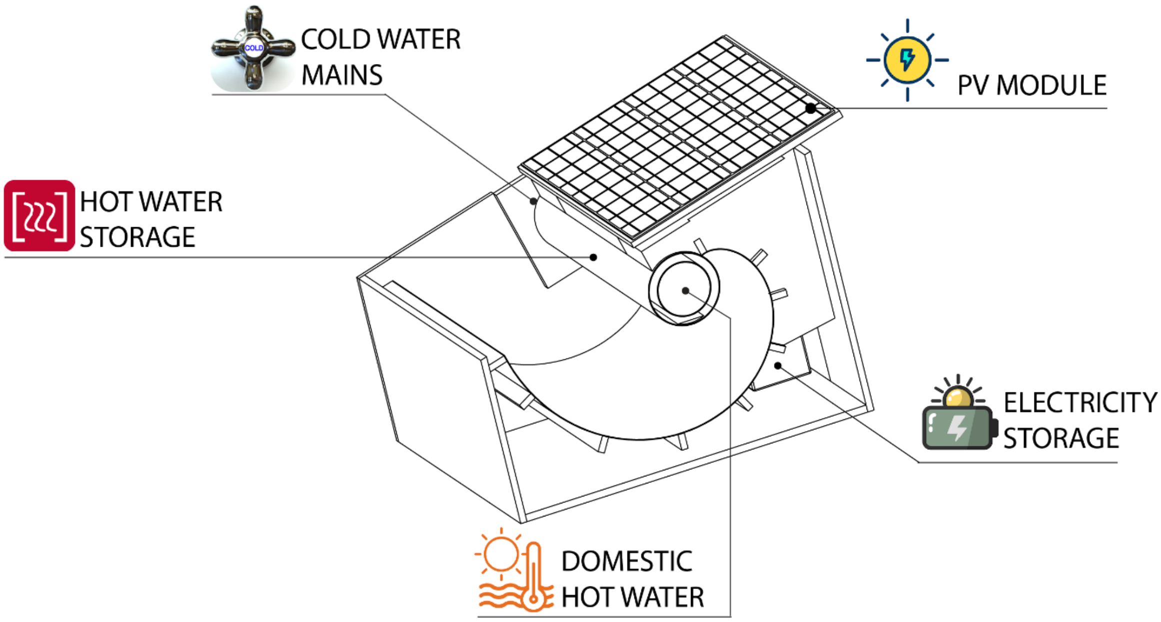

Fig. 1. The modular Asymmetric Formed Reflector with Integrated Collector and Storage (AFRICaS) Partially Hybridised Solar Technology (PHST) concept [44,45].

2. Technical specification of the AFRICaS PHST components

2.1. The thermal diode AFRICaS ICSSWH subsystem

Researchers at Ulster University have been developing various vertical [46,47] and horizontal [34,42,48] types of thermal diode ICSSWH devices in cylindrical and planar formats. Cylindrical versions have storage tank vessel diameters ranging from 150 mm to 360 mm and hot water storage volume ranging from 16.5 L to 30.8 L for system lengths ranging from 1 m to 1.63 m. A readily available thermal diode ICSSWH device with a volume capacity of 16.7 L and system length of 1 m, provided the needed modularity to the AFRICaS PHST concept as a sufficient entry-level unit. Growing hot water demands would be met by scaling up using multiple identical units connected in series or in parallel.

2.2. PV subsystem components

The power rating of the PV module was estimated using the daily electrical demand of $E_L = 250\ \mathrm{Wh/day}$ (see Table 1) by considering the lowest monthly average daily Global Horizontal Irradiation. The lowest monthly average daily irradiation for the selected location in Uganda at Busitema University (Latitude = 0.547163°N, Longitude = 34.019773°E), Tororo district is $H(\beta = 0°) = 5.25\ \mathrm{kWh/m^2/day}$ and occurs in July [49]. Tilted south facing surface solar radiation modelling utilised the Isotropic Sky Model [50–52] which considers beam, isotropic diffuse and ground reflected components. Using a ground reflectance of 0.2 (sand/dry grass) and the diffuse fraction empirical formulation in Eq.(1), the estimated monthly average daily solar irradiation incident on the aperture tilt angle of 15° of the south facing AFRICaS PHST prototype [45] is $H_T(\beta = 15°) = 4.61\ \text{kWh/m}^2\text{/day}$. Other mixed approaches [53] to derive the solar energy potential at a site could be considered.

$$F_{\text{Dm}} = 1 - 1.13K_{\text{Tm}} \tag{1}$$

where F_{Dm} is the diffuse fraction of the monthly average daily global horizontal irradiation and K_{Tm} is the clearness index for each month.

According to the PV module sizing approach by Labouret and Villoz [54] the current at Maximum Power Point (MPP) and Standard Test Conditions (STC) is estimated using Eq.(2).

$$I_{\text{m}} = \frac{Q_L}{H_T \cdot \eta_B \cdot \eta_{CC} \cdot \eta_{wire} \cdot DF} \tag{2}$$

where Q_L is the electric charge equivalent of energy supplied to the load for specified 12 V DC system in Ah/day, i.e., $Q_L = E_L/12$ and H_T is the monthly average daily solar radiation incident on the tilted PV module surface in $\text{kWh/m}^2\text{/day}$. Assuming battery charging efficiency ($\eta_B = 0.95$), charge controller efficiency ($\eta_{CC} = 0.98$), dust/dirt/sand factor ($DF = 0.9$) and wiring effectiveness ($\eta_{wire} = 0.97$), the estimated $I_{\text{m}} = 5.55$ A. Finally, the peak power of the PV module was obtained using Eq.(3).

$$\text{P}_{\text{m}} = I_m \times \text{V}_m \tag{3}$$

where V_m is PV module's voltage at MPP, i.e., typically $17\ \text{V} \leq \text{V}_{\text{m}} \leq 18$ V for a 12 V system located in hot climate [54]. This results in PV module peak power values in the range $94.4\ \text{V} \leq \text{P}_{\text{m}} \leq 100.0$ W. One ECO-WORTHY 100 Wp polycrystalline PV panel (36 PV cells and effective PV cell surface area of $0.584\ \text{m}^2$) was selected.

Battery sizing considered 2 days of autonomy, a maximum DOD of 75% for sufficient storage during cloudy days and at night and a battery discharge efficiency, η_{disch}, of 85% according to Eq.(4). One maintenance free Valve Regulated Lead Acid (VRLA) Sonnenschein 12 V battery, model GF1252YO of gel technology with a C_{20} rating of 60 Ah was selected.

$$\text{Battery capacity (Ah)} = \frac{\text{daily load (Wh)} \times \text{days of autonomy}}{\text{System voltage (V)} \times \text{DOD} \times \eta_{disch}} = \frac{250\ \text{Wh} \times 2}{12 \times 0.75 \times 0.85} = 65.4\ \text{Ah} \tag{4}$$

The charge controller should support the full short circuit current of the connected PV panel [55]. A safety margin multiplier of 1.3 [56] on the PV panel short circuit current (I_{SC}) determined a commercially available 12 V/10 A charge controller for the PV subsystem. Two charge controller technologies were selected as detailed in Table 3 to evaluate their benefit towards electrical energy yield of the PV subsystem.

Table 3
The selected Victron PWM-Pro and MPPT SmartSolar charge controllers in the PV subsystem of the AFRICaS cogeneration prototype.

Parameter	Unit	PWM-Pro	MPPT SmartSolar
Unit cost	USD $	54.0	140.0
Maximum battery current	A	10	10
Nominal PV power, 12 V	W	-	145
Automatic load disconnect	A	-	15
Peak efficiency	%	-	98
Self-consumption	mA	<10	20
Absorption charge	V	14.4	14.4
Float charge	V	13.8	13.8
Equalisation charge	V	14.6	-
Low voltage load disconnect	V	11.1	Battery life algorithm
Low voltage load reconnect	V	12.6	Battery life algorithm
Temperature compensation	mV/°C	-	-16/32

3. Experimental methodology and set-ups

The modular AFRICaS PHST prototype was evaluated at the Centre for Sustainable Technologies (CST), Ulster University using a state-of-the-art indoor Solar Simulator [57] while adhering to the ISO 9806:2017 [58] standard. The solar simulator has 35 metal halide lamps fitted with collimating lenses that radiate light across an infrared filtering medium to achieve a light output comparable to the AM1.5 daylight reference spectrum. The solar simulator was tilted to an angle of 15° to the horizontal (measured using a digital inclinometer (FISCO Solatronic) with ±0.2° accuracy) to produce a light beam normal to the aperture of each subsystem.

Partial hybridity of the prototype was exploited by testing the individual subsystems using separate experimental rigs to overcome space constraints under the solar simulator, i.e., one for the thermal AFRICaS subsystem and the other for the PV subsystem. The measured intensity on the subsystems' aperture varied in the range $640 - 775 \text{ W/m}^2$. This range is typical of the average hourly total solar radiation incident on a south facing surface at a 15° tilt angle during a 6 h period (between 10:00 a.m. to 4:00 p.m) of utilisable solar energy for most locations in Sub-Saharan Africa. Each solar energy collection experiment was carried out under constant solar radiation for a period of six hours and static air conditions. The measurement system for simulated solar irradiance consisted of a pyranometer (Kipp & Zonen-CM11) of sensitivity $4.66\ (\mu\mathrm{V/W})\mathrm{m}^2$ connected to a handheld digital multimeter (Mastech MAS830L).

The total solar energy $E_{\mathrm{Sim}\to\mathrm{ICS}}$ and $E_{\mathrm{Sim}\to\mathrm{PV}}$ received on the apertures of the AFRICaS ICSSWH subsystem and the PV module, respectively during the exposure period were determined according to Eq.(5) and Eq.(6).

$$\text{Energy supplied by solar simulator in J } (E_{\mathrm{Sim}\to\mathrm{ICS}}) = G_{\mathrm{avg}} \mathrm{A_p} \Delta t \tag{5}$$

where G_{avg} is the average measured simulated solar intensity on the aperture and $\mathrm{A_p}$ the aperture surface area of the AFRICaS ICSSWH subsystem (i.e., $0.45\ \mathrm{m}^2$) and the duration of simulated irradiance, $\Delta t = 21{,}600$ s.

$$\text{Energy supplied by solar simulator in Wh } (E_{\mathrm{Sim}\to\mathrm{PV}}) = G_{min} \mathrm{A_{PV}} \Delta t \tag{6}$$

where G_{min} is the minimum irradiance measured on the PV cell surface, $\mathrm{A_{PV}}$ is the effective surface area of module PV cells and $\Delta t = 6$ h.

Hot water draw-off simulations utilised a demand profile proposed by Prinsloo [21] which provides ~28 L per day for a 4-person rural household. For electricity demand, field study data measured at an off-grid teacher's house of the SolaFin2Go project [32] by Ulster University at Jamataka Primary School in Botswana was utilised. The data covered at least 100 days during the period October 2018 to March 2019. The electrical load consisted of lighting, phone charging, a television set and its powered receiver and converter, and a small fan. The average electrical demand was $563 \pm 114\ \mathrm{Wh/day}$ and the television's power converter and night phone charging constituted the baseline load over the 24 h period. Fig. 6 and Fig. 7 show the respective hot water draw-off and electrical demand profiles, derived for this experimental simulation methodology.

3.1. Experimental rig set-ups and sensor locations

Fig. 2. depicts the schematic layout of the experimental rig for the AFRICaS ICSSWH subsystem enclosing the cylindrical thermal diode ICSSWH prepared as described in previous work [34,48]. It highlights instrumentation, pipework, isolation valves, and auxiliaries,

allowing low pressure mains freshwater supply below 1 bar to avoid compromising the integrity of the ICSSWH seals.

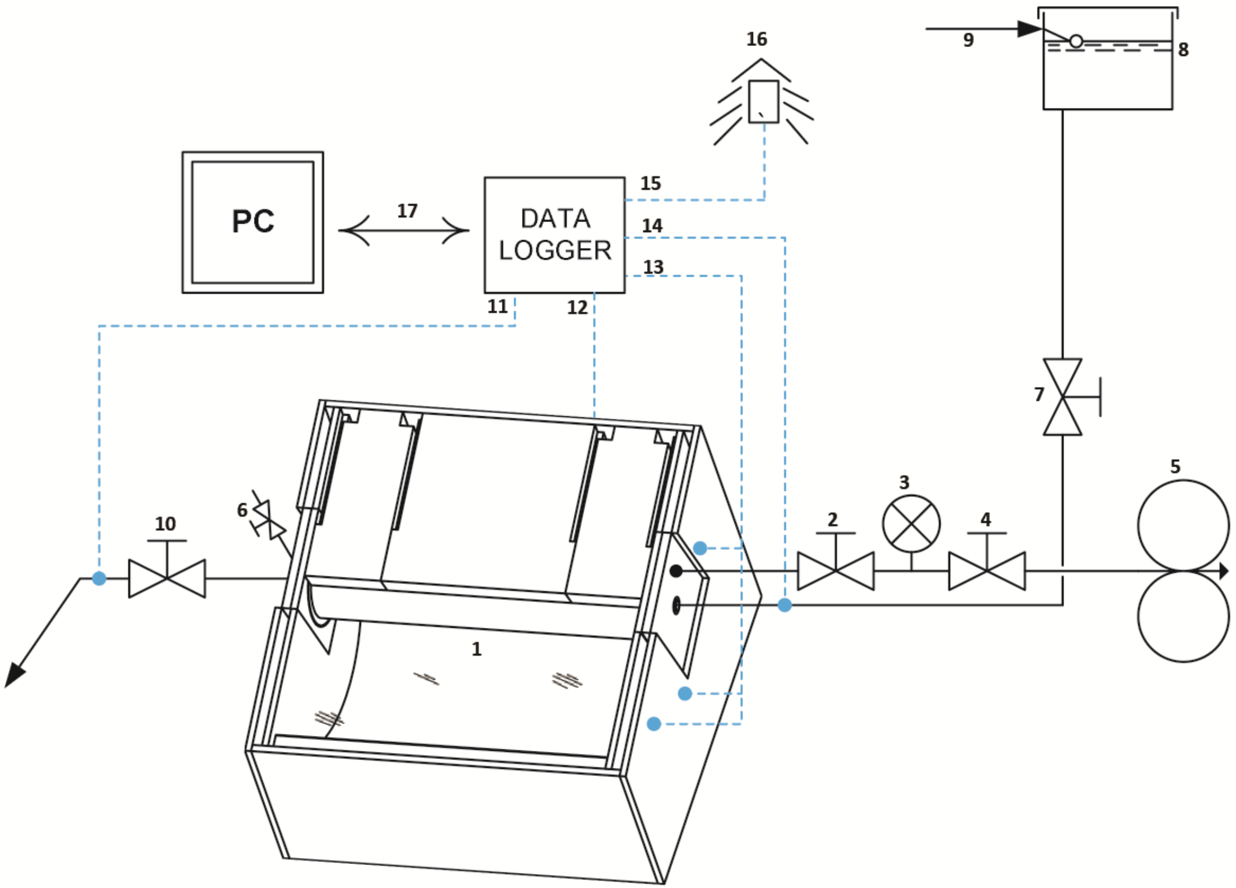

1. AFRICaS ICSSWH
2. Vacuum shutoff valve
3. Pressure gauge
4. Vacuum pump isolation valve
5. Vacuum pump (oil rotary vane single-stage)
6. System vent valve
7. System cold feed valve
8. Overhead cold-water storage tank
9. Mains water supply
10. System outlet/drain valve
11. Outlet hot water temperature
12. Collector temperatures (water in tank and absorber)
13. Air temperature in reflector cavity
14. Cold water inlet temperature
15. Ambient air temperature
16. Ambient temperature sensors
17. PC-data logger link

Fig. 2. Experimental setup and instrumentation for indoor draw-offs.

Temperature measurement utilised 19 thermocouple sensors (T-type Copper/Constantan) with ±0.5 K accuracy. Fig. 3. shows the temperature sensor locations on the AFRICaS ICSSWH subsystem experimental rig in cross-section. The thermocouples linked onto various channels of a Delta-T DL2e data logger, which sampled every 5 s and recorded average temperatures on 5-min intervals. The data logger stored continuous temperature records for the a. absorber, b. air enclosed in the reflector cavity, c. water in the water storage vessel; d. air enclosed in the lead acid battery compartment at the back of the reflector, e. mains freshwater inlet and f. the hot water outlet. Moreover, temperature measurements of laboratory ambient air, hot water in storage, absorber, and air enclosed in reflector cavity utilised multiple temperature sensors for improved measurement accuracy. Table 4 describes the various thermocouple locations on the prototype and in the laboratory environment.

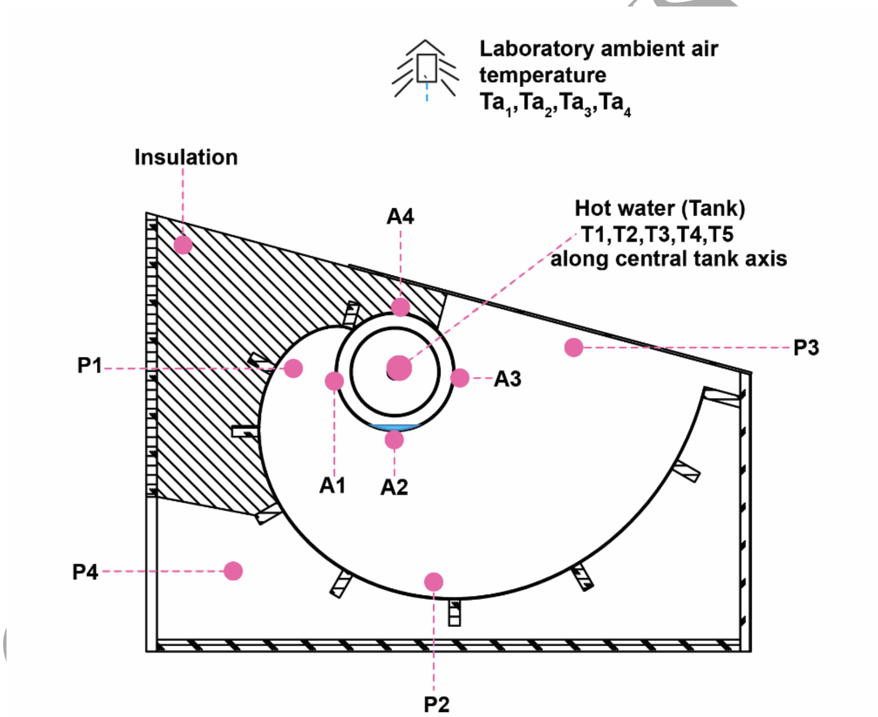

Fig. 3. Temperature sensor locations on the AFRICaS ICSSWH subsystem experimental rig.

Table 4
Temperature measurement locations on the AFRICaS ICSSWH subsystem experimental rig

Measurement location	Measurement quantity	Labels and descriptions
Absorber	Temperature of the absorber surface	Back, **A1** Bottom, **A2** Front, **A3** Top, **A4**
Air enclosed in the reflector cavity		Hot air cavity, **P1** Above reflector, **P2**

Measurement location	Measurement quantity	Labels and descriptions
	Temperature of the air enclosed in the reflector cavity	Below glazing, **P3**
Water in the storage tank of the ICSSWH	Temperature of water in ICSSWH tank	Five sensors distributed equidistant along the central axis of the water filled tank, **T1**, **T2**, **T3**, **T4**, **T5**
Air enclosed in the proposed lead acid battery compartment at the back of the reflector	Temperature of the proposed battery compartment	One temperature sensor in the proposed battery compartment, **P4**
Laboratory ambient	Ambient air temperature	Four temperature sensors in ambient around the prototype
Mains fresh water	Mains freshwater inflow temperature	One temperature sensor on inlet copper pipe (#14 on Fig. 2)
Hot water outlet	Hot water outflow temperature	One temperature sensor on outlet copper pipe (#11 on Fig. 2)

Fig. 4 shows a photograph of the AFRICaS ICSSWH subsystem experimental rig in the laboratory. Hot water draw-offs utilised manual flow volume measurements that employed a stopwatch, graduated measuring jugs and a bucket. Hot water discharged through the outlet hose into the bucket as mains freshwater simultaneously entered the storage vessel at the inlet. For continuous measurements, a T-type thermocouple in contact with the copper outlet port provided a sufficient measurement of hot water temperature exiting the storage vessel. A stop clock enabled recording of the duration for the system to deliver the required hot water volume into the bucket. A digital thermometer (Tenma 72-7715) read and recorded temperature measurements of mixed hot water draw-off samples using a T-type thermocouple. The actual volume of extracted hot water draw-off samples was measured using a graduated measuring jug to estimate the flow rate in L/min for each draw-off event. Finally, T-type thermocouples placed along the centreline of the storage water vessel measured the temperature of the water in the storage water vessel, enabling the estimation of the thermal energy extracted for each draw-off.

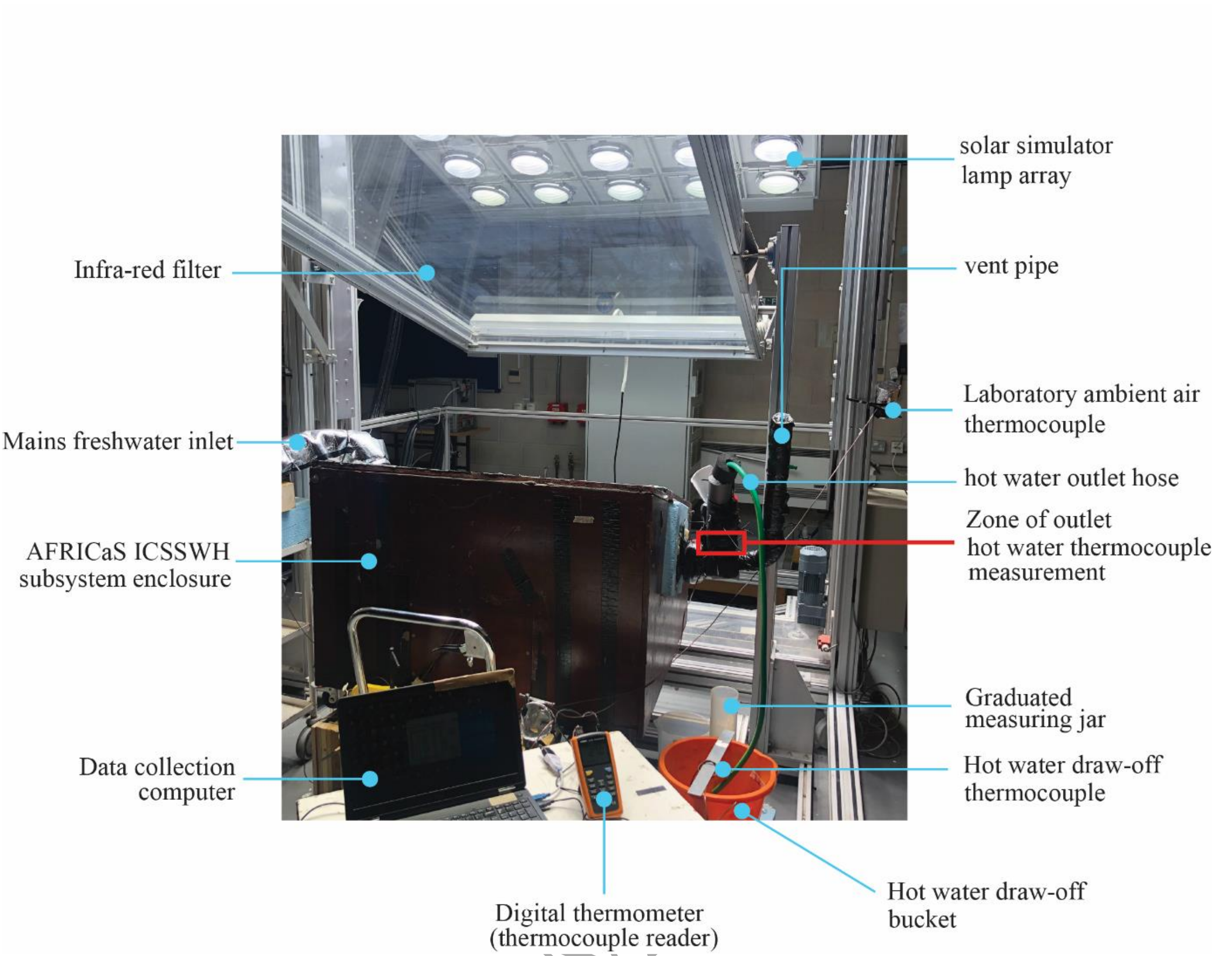

Fig. 4. The AFRICaS ICSSWH subsystem undergoing experimental hot water draw-off simulations in the laboratory.

Fig. 5 shows the experimental rig for the PV subsystem and the set-up used for simulating electricity demand in the laboratory. The setup ensured that the two types of charge controllers i.e., a Pulse Width Modulation (PWM) and a Maximum Power Point Tracking (MPPT) selected in Table 3 were used interchangeably for comparison purposes. T-type thermocouples attached in four locations at the back of the PV module measured the PV module temperature. Additionally, two T-type thermocouples measured ambient air temperature in the laboratory near the test rig. A custom-built Current-Voltage Measurement Interface (CVMI) enabled the measurement of all electrical parameters using potential dividers and shunt resistors to transform the true voltage and current values into a millivolt scale range for compatibility with the datalogger. The custom-built CVMI linked to the datalogger through three 4-core shielded signal cables. Measured electrical parameters included the operating voltage and current for the PV module, the VRLA battery, and the load. Continuous recording of electrical and temperature measurements utilised an Omega OM-DAQXL data logger which recorded a single average value of 12 samples every minute.

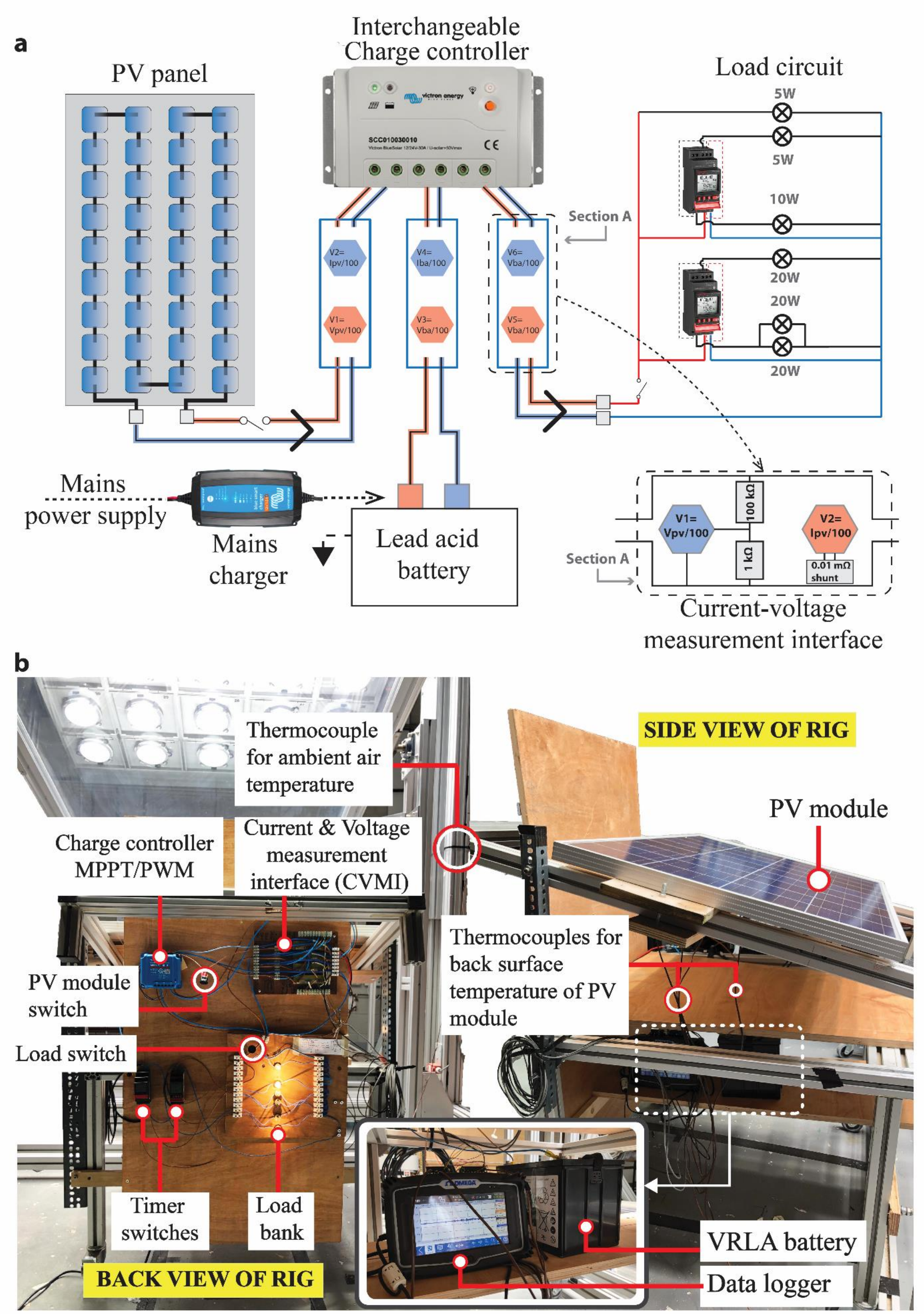

Fig. 5. Setup of the PV subsystem showing (a) the system schematic for measurement of electrical parameters and simulating the electrical demand profile and (b) the photograph of the experimental rig in the laboratory.

Current and voltage measurements were used to determine the energy yield metrics from the PV module during the 6 h exposure period of simulated irradiance. Energy yield of the PV module and the corresponding average efficiency were derived according to Eq.(7) and Eq.(8) , respectively. Performance evaluation of the PV subsystem considered all cells exposed to a minimum irradiance G_{min}. Slightly higher irradiances measured on certain cells would not be expected to significantly influence electrical yield because current flow through the module (formed of PV cells interconnected in series) would be limited by those PV cells subjected to the lowest irradiances. The energy supplied to the load during each 24 h period was derived using Eq.(9).

$$\text{PV energy yield in Wh } (E_{\text{PV}}) = \sum_{0}^{360} \frac{V_{\text{PV}} \times I_{\text{PV}}}{60} \tag{7}$$

$$\text{PV module efficiency } \eta_{\text{PV}} = \frac{E_{\text{PV}}}{E_{\text{Sim}\rightarrow\text{PV}}} = \frac{\sum_{0}^{360} \frac{V_{\text{PV}} \times I_{\text{PV}}}{60}}{G_{min} \text{A}_{\text{PV}} \Delta t} \tag{8}$$

$$\text{Energy supplied to the load in Wh } (E_L) = \sum_{0}^{1440} \frac{V_L \times I_L}{60} \tag{9}$$

where V_{PV} and I_{PV} are the measured voltage and current produced by the PV module and V_L and I_L are the voltage and current drawn by the load. Initially, a Victron Blue Smart IP65 Mains Charger was utilised to achieve a full state of charge of the battery, determined when charging status of the LED indicator displayed the "STORAGE" state. The fully charged battery was rested for a period of 12 h between tests to establish a common initial condition of battery state of charge for each experimental simulation of the PV subsystem.

3.2. Simulated hot water draw-off patterns and electricity demand

To evaluate the thermal energy output of the AFRICaS ICSSWH subsystem, the study derived simplified hot water draw-off patterns based on the hot water demand profile suggested by Prinsloo [21]. Fundamentally, the AFRICaS ICSSWH subsystem is a batch solar water heater which may also function as a preheater. As a batch solar water heater, it collects and stores solar energy in hot water during the day for later use. In this mode, hot water demand comprises intensive warm water withdrawal from the system in the evening and/or morning hours when sunlight is insufficient to activate the thermal diode. The derived hot water draw-off patterns were simulated for three scenarios:

- Scenario 1: High intensity draw-offs during the collection (sunny daytime) period only
- Scenario 2: High intensity draw-offs at the end of collection period
- Scenario 3: Distributed draw-offs throughout the day

Fig. 6 presents the three hot water draw-off scenarios indicating their reationship to the 6 h simulated solar radiation exposure period selected as noon ± 3 h (i.e., 9:00-15:00 h) at $730\,\mathrm{W/m^2}$ on the aperture of the AFRICaS ICSSWH subsystem. Scenario 1 (Fig. 6a) shows a draw-off pattern of 28 L consisting of 5 separate events occurring over a short midday period (approximately 1 h and 40 min). This may be likened to simultaneous coexistance of an intensive demand for preheated hot water during preparation of lunchtime meals and solar energy collection in the middle of the day. Scenario 2 (Fig. 6b) shows a draw-off pattern of 28 L, again consisting of 5 separate events during a period of 1h 40 min, but this time occuring immediately after the solar collection period. This maybe likened to a high intensity demand for preheated water in the evening after sunset (e.g., for bathing). Finally, Scenario 3 (Fig. 6c) shows a distributed draw-off pattern of a total of 28 L during the day from morning to evening. This draw-off pattern is the closest in similarity to Prinsloo's [21] except that there are no draw-offs during the night.

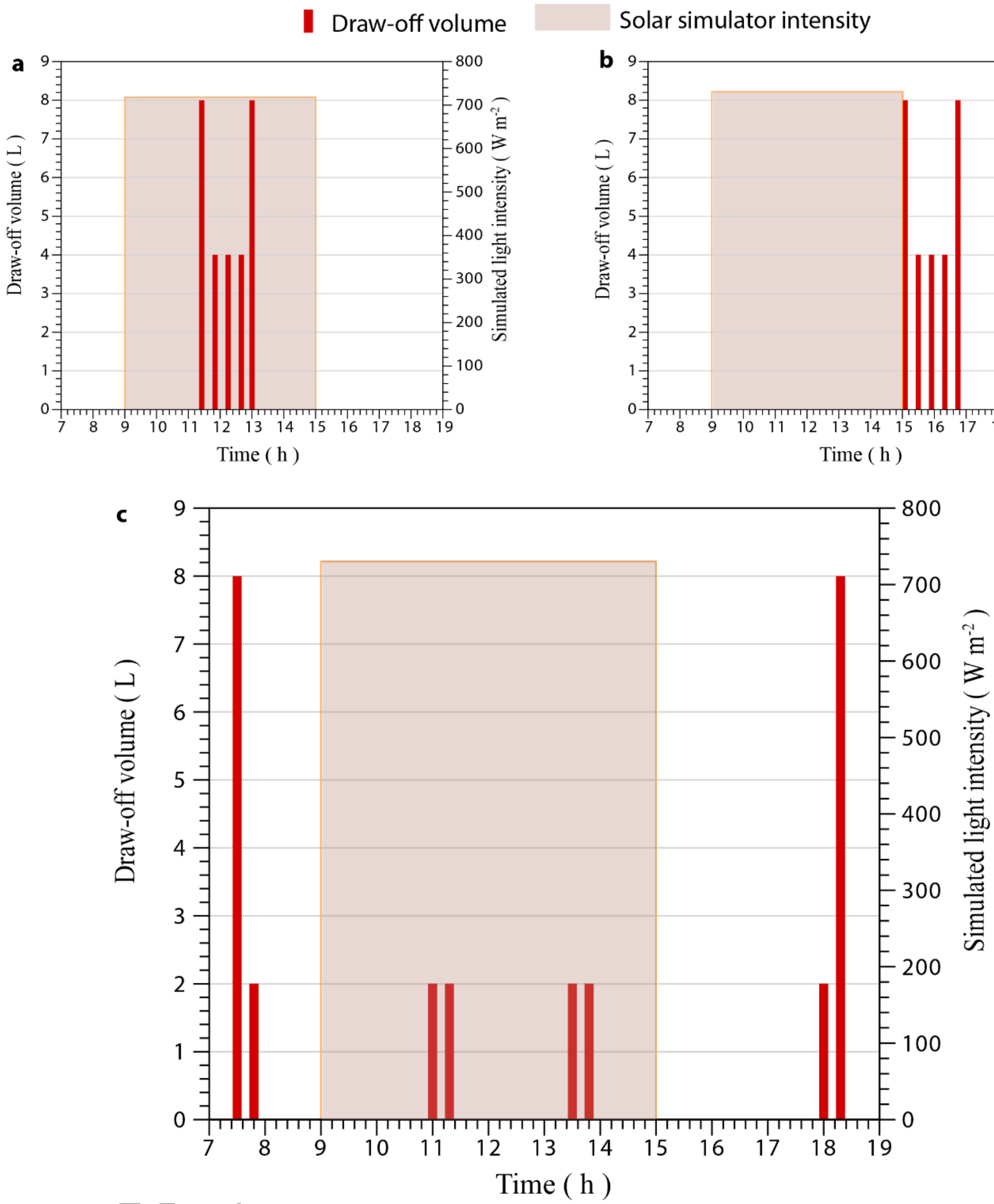

Fig. 6. Three scenarios for experimental simulation of hot water draw-off (a) high intensity draw-off pattern during the collecting period-Scenario 1 (b) high intensity draw-off pattern after the collecting period-Scenario 2 and (c) distributed draw-offs during the day-Scenario 3.

Hot water draw-off produces a temperature drop in the thermal store (i.e., the hot water in the inner storage vessel) from which the amount of thermal energy extracted ($\mathrm{Q_{HW}}_j$) can be calculated for each draw-off, j, using Eq.(10),

$$\mathrm{Q_{HW}}_j = \mathrm{m_w} C_{\mathrm{p,w}} \left(T_{\mathrm{w,i}} - T_{\mathrm{w,f}}\right)_j \tag{10}$$

where $C_{\mathrm{p,w}}$ is the specific heat capacity of water at constant pressure whilst $\left(T_{\mathrm{w,i}} - T_{\mathrm{w,f}}\right)_j$ is the temperature change of the storage vessel water volume for each single draw-off from the average initial temperature measurement $T_{\mathrm{w,i}}$ to the average final temperature measurement $T_{\mathrm{w,f}}$ before and after each draw-off, respectively. The mass of water in the inner storage vessel, $\mathrm{m_w}$ was determined using Eq.(11),

$$\mathrm{m_w} = \rho v_t \tag{11}$$

where ρ the density of water, v_t the volume of the inner storage vessel. The density, ρ and specific heat capacity, $C_{\mathrm{p,w}}$ of water were evaluated at the average temperature of $T_{avg} = \left(T_{\mathrm{w,i}} + T_{\mathrm{w,f}}\right)/2$ using the normative formulae provided in the Annex C of ISO 9806:2017 for liquid water in the range up to 12 bar and $0 < T_{avg} < 185\ ℃$. Finally, in the case of the AFRICaS ICSSWH subsystem, the average solar thermal collection efficiency, η_{Th} for the 6 h exposure period of simulated solar irradiance was determined from Eq.(5) and Eq.(10), using Eq.(12),

$$\eta_{Th} = \frac{\sum_{j=1}^{N} \mathrm{Q_{HW}}_j}{G_{\mathrm{avg}} \mathrm{A_p} \Delta t} \tag{12}$$

where N refers to the individual draw-offs i.e., $N = 5$ in Scenario 1 and 2, and $N = 8$ in Scenario 3.

The electrical energy output of the AFRICaS PHST was evaluated experimentally using an automatic load bank circuit that simulated the electrical demand profile. The load consisted of an array of halogen lamps (2 x 5W, 1 x 10W and 3 x 20W) connected to four programmable channels of two 12 V Digital DIN Rail timer switches to achieve automatic switching of the lamps, as shown in Fig. 5a. The simulated experimental load profile is compared against the load profile derived from measured electrical consumption data of the teacher's house in the SolaFin2Go project [32] as shown in Fig. 7. Automatic lamp switching over a 24 h period resulted in a daily simulated experimental electrical demand of 570 Wh/day which was broadly similar to the consumption profile derived from SolaFin2Go field data.

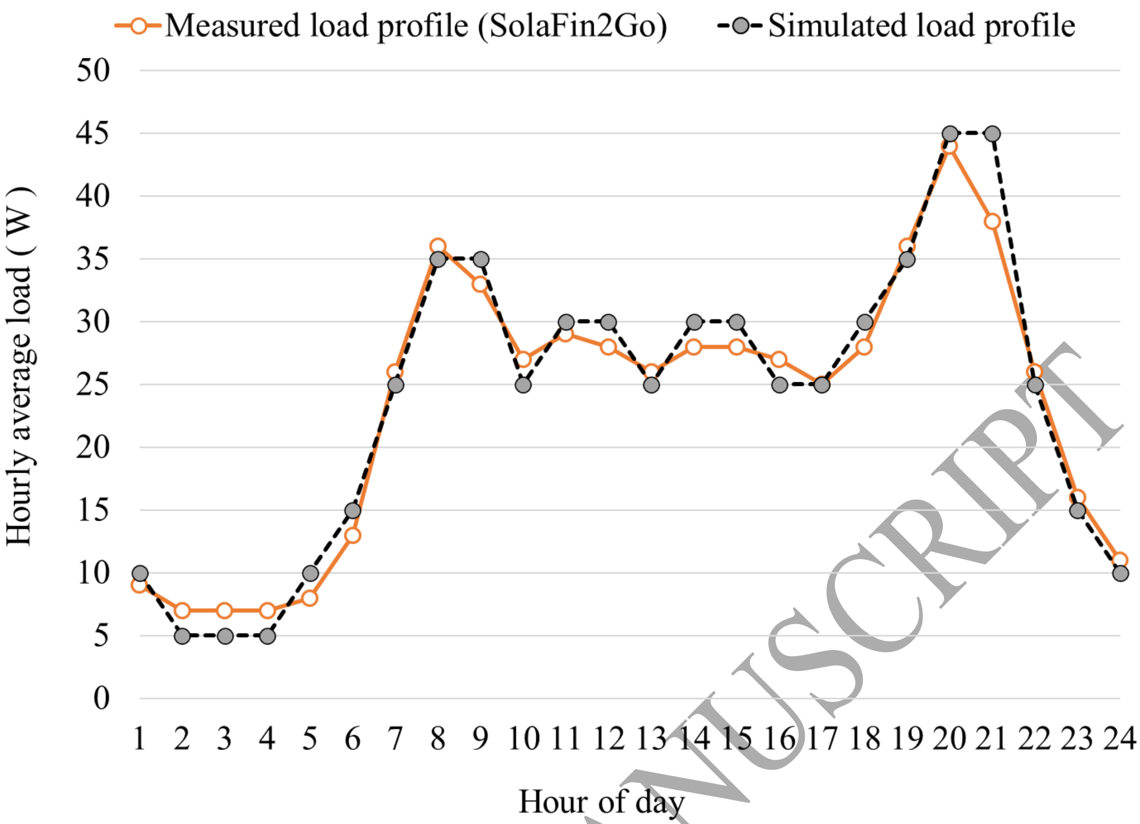

Fig. 7. Comparison of the simulated load profile and the electrical consumption profile measured at the teacher's house in the SolaFin2Go project [32] in Jamataka, Botswana.

Multi-day tests were performed to evaluate the behaviour of the AFRICaS PHST prototype under simulated hot water demand for the three scenarios and simulated electrical demand for each selected charger controller. For hot water draw-offs under scenario 3, the AFRICaS ICSSWH sat without collection on the day prior to the first simulation day. Therefore, results presentation ignored the first simulation day because initial draw-offs in the morning would be meaningless, unless the preceding day was notionally considered a very cloudy day.

4. Results and discussion

4.1. Hot water draw-off simulations

Fig. 8. Multi-day shows the measured temperature variations for the investigated multi-day test scenarios indicating the effect of draw-offs conducted at the same time on different days. The temperature variation of the absorber, air enclosed in the reflector cavity, storage hot water and laboratory ambient air represents averaged data at multiple points. Measured temperature data of mains fresh water (inlet) and hot water outlet are shown only for periods of simulated draw-off events. The measured average simulated instensity on the two testing days of scenarios 1, 2 and 3 was $718 \pm 35\,\mathrm{W/m^2}$, $730 \pm 25\,\mathrm{W/m^2}$ and $732 \pm 24\,\mathrm{W/m^2}$, respectively. Laboratory

ambient temperature during the testing period of scenarios 1, 2 and 3 varied between ~18-26°C, ~19-26°C and ~18-27°C, respectively, typical of countries in the tropical zone. Draw-offs influence the storage water temperature and the temperature of the absorber and enclosure cavity air inside the prototype. Apparently, utilising hot water during the collection period (Scenario 1) has the greatest benefit of overnight warm water retention, which results in a relatively higher storage water temperture on the morning of the next day. There are significant temperature variations in the mains freshwater (inlet) temperature with time, typically ~26-33 °C initially (i.e., standing water contained within the pipes located in the laboratory space at ambient temperature) falling to ~16-20 °C (i.e., mains freshwater from underground pipes).

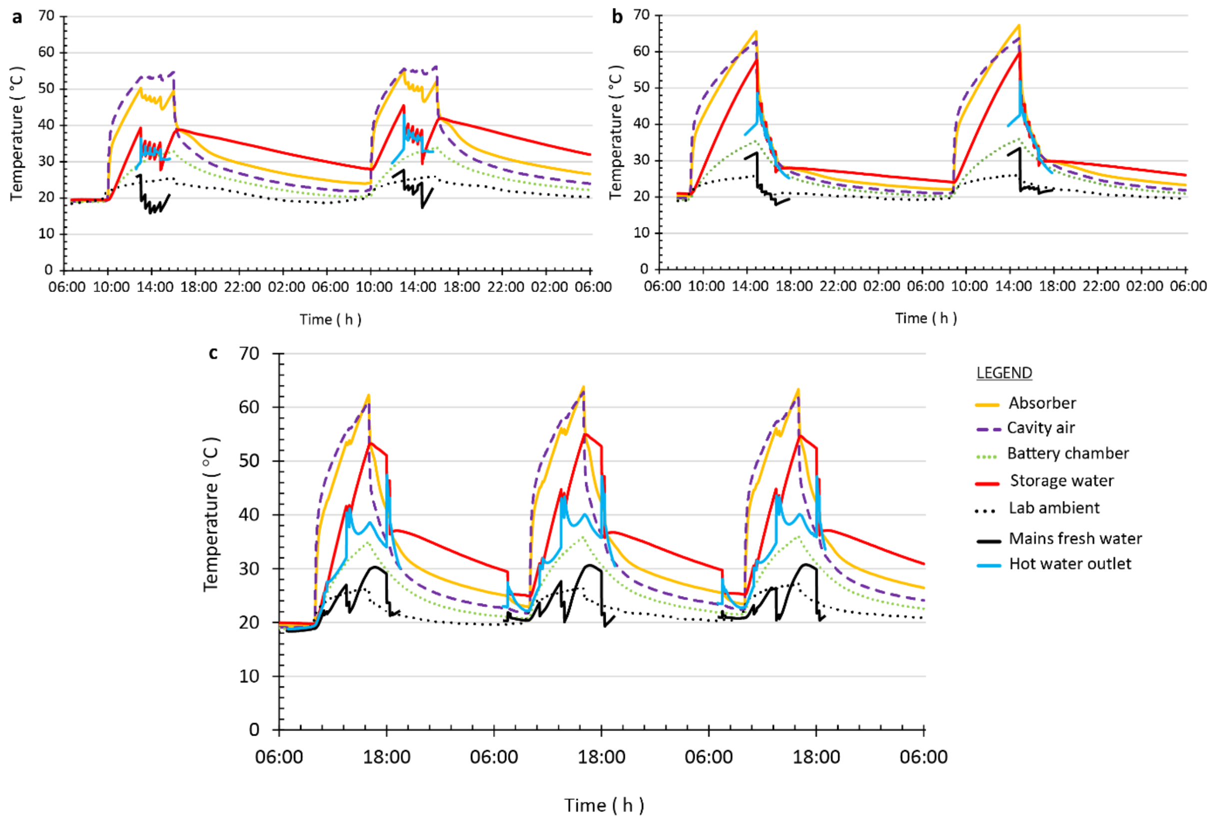

Fig. 8. Multi-day temperature variations of experimental simulation showing tests with: (a) high intensity draw-offs during the collecting period – Scenario 1; (b) high intensity draw-offs at the end of the collection period – Scenario 2; and (c) distributed draw-offs at different times of the day – Scenario 3.

Experimental draw-off simulations provide insight about the estimated collector performance in terms of hot water delivery throughout the day. Fig. 9 shows the mixed hot water temperature in the bucket for each draw-off of the simulated scenarios on day 1 (left hand side) and day two (right hand side) in relation to the time of day. Scenario 3 produced the worst consistency in hot water temperature and its last four draw-offs (afternoon and evening) have a higher hot water temperature than the first four (during morning hours) due to nighttime heat losses from the store. Scenario 2 produces the greatest decline in hot water temperature after each draw-off. Scenario 1 delivers the greatest temperature consistency for each draw-off. The timing of draw-offs has a significant effect on the temperature of delivered hot water. Early morning draw-offs delivered water at 27°C whereas early evening draw-offs delivered water at 43°C.The best hot water use pattern depends on the application but users would certainly prefer a system that delivers hot water at a consistent temperature.

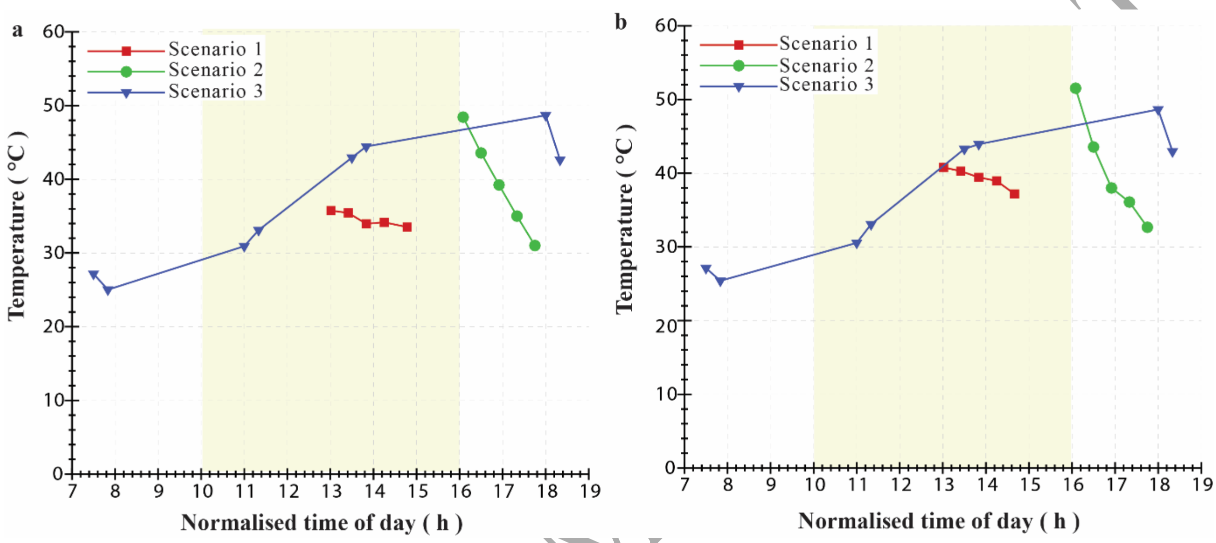

Fig. 9. Mixed water temperature in the bucket for each draw-off in scenarios 1, 2 and 3, respectively on Day 1 (left hand side) and Day 2 (right hand side).

Table 5, 6 and 7 summarise the total energy extracted from the AFRICaS ICSSWH subsystem for the individual testing days along with draw-off flow rates and the storage water temperatures measured in the tank before and after each draw-off. The hot water temperature delivered by the prototype across the two simulated days ranged between ~33.5-40.8 °C , ~31.0-51.5 °C and ~25.02-48.68 °C, for scenarios 1, 2 and 3, respectively. The initial and final storage water temperatures before and after each draw-off are relatively higher on the second day. The initial storage water temperature before draw-offs on both days varried between ~35-46°C, ~33-60°C and ~26-53°C for scenarios 1, 2 and 3, respectively. Conversely, the final storage water temperature after draw-offs on both days varried between ~28-36°C, ~28-46°C and ~25-47°C for scenarios 1, 2 and 3, respectively. The quantity of heat energy extracted appears to be independent of the draw-off pattern. For the total actual measured hot water volume delivered by the system ranging from 28.0 L to 30.8 L, the amount of heat energy delivered ranged between 1,954 kJ and 2,133 kJ across the scenarios with an average of 2,074±75 kJ. Finally, the solar thermal conversion efficiency for the different hot water draw-off simulation days ranged from 28.0% to 30.6% with an average of $29.4 \pm 1.0\%$. The consistency in the heat energy extracted and collection efficiency in all scenarios indicates a substantial degree of predictability of the current experimental methodology.

Table 5
Heat energy delivered by the AFRICaS ICSSWH subsystem for the simulated draw-offs in Scenario 1.

	Time of draw-off	Actual draw-off volume (L)	Draw-off duration (s)	Flow rate (L/min)	Storage water temperature (°C)		Draw-off mixed water temperature (°C)	Energy extracted, Q_{HW_j} (kJ)
					Before draw-off ($T_{w,i}$)	After draw-off ($T_{w,f}$)		
DAY 1	13:01	8.0	214.0	2.2	39.3	31.3	35.7	554.7
	13:25	4.0	66.3	3.6	35.7	31.6	35.4	282.2
	13:50	4.0	54.8	4.4	35.4	30.9	34.0	310.4
	14:15	4.0	36.7	6.6	34.9	30.7	34.2	285.9
	14:47	8.0	63.4	7.5	35.3	27.8	33.5	520.8
		28.0	**435.2**	**4.9**				**1,954.0**
DAY 2	13:01	8.5	217.2	2.4	45.5	36.4	40.8	632.6
	13:25	4.2	42.0	6.0	40.4	36.2	40.3	291.5
	13:50	4.1	54.5	4.6	39.7	35.5	39.4	294.9
	14:15	3.9	64.1	3.7	38.9	34.9	38.9	278.7
	14:40	8.4	82.5	6.1	38.7	29.6	37.2	635.3
		29.1	**460.3**	**4.5**				**2,133.1**

Table 6

Heat energy delivered by the AFRICaS ICSSWH subsystem for the simulated draw-offs in Scenario 2.

	Time of draw-off	Actual draw-off volume (L)	Draw-off duration (s)	Flow rate (L/min)	Storage water temperature (°C)		Draw-off mixed water temperature (°C)	Energy extracted, Q_{HW_j} (kJ)
					Before draw-off ($T_{w,i}$)	After draw-off ($T_{w,f}$)		
DAY 1	14:55	8.1	110.3	4.4	57.7	45.6	48.4	834.3
	15:20	4.4	59.1	4.4	45.7	40.4	43.6	367.7
	15:45	4.3	50.2	5.1	40.6	36.1	39.2	311.5
	16:10	4.2	57.3	4.4	36.2	32.4	35.0	262.3
	16:35	8.4	93.5	5.4	32.6	27.8	31.0	332.12
		29.3	**370.4**	**4.7**				**2,108.0**
DAY 2	14:55	8.5	117.1	4.4	59.8	45.3	51.5	994.6
	15:20	4.2	56.3	4.5	45.6	40.6	43.5	341.4
	15:45	4.0	54.9	4.4	40.7	36.7	39.8	272.6
	16:10	4.2	60.7	4.1	36.9	33.8	36.1	212.7
	16:35	8.5	100.9	5.1	34.0	29.7	32.7	297.3
		29.3	**389.8**	**4.5**				**2,118.6**

Table 7

Heat energy delivered by the AFRICaS ICSSWH subsystem for the simulated draw-offs in Scenario 3.

	Time of draw-off	Actual draw-off volume (L)	Draw-off duration (s)	Flow rate (L/min)	Storage water temperature (°C)		Draw-off water temperature (°C)	Energy extracted, Q_{HW_j} (kJ)
					Before draw-off ($T_{w,i}$)	After draw-off ($T_{w,f}$)		
DAY 2	07:30	8.3	118.9	4.2	29.4	25.7	27.2	258.8
	07:50	2.4	37.0	3.9	25.8	25.2	25.0	46.8
	11:05	2.4	42.7	3.4	30.9	29.5	30.9	102.4
	11:25	2.5	37.8	4.0	32.0	30.4	33.1	108.9
	13:30	2.3	39.4	3.5	44.7	41.6	42.9	212.4
	13:50	2.3	35.6	3.8	44.0	40.8	44.4	222.6
	18:00	2.3	39.8	3.5	52.7	47.1	48.7	389.6
	18:20	8.3	104.4	4.8	47.1	35.8	42.6	781.7
		30.8	**455.5**	**3.9**				**2,123.2**
DAY 3	07:30	8.5	115.6	4.4	29.7	25.7	27.1	276.7
	07:50	2.3	38.2	3.7	26.1	25.4	25.4	50.0
	11:00	2.4	36.9	3.9	30.5	29.2	30.5	94.5
	11:20	2.2	36.4	3.7	31.6	30.3	33.1	88.1
	13:30	2.2	36.2	3.7	44.8	41.3	43.3	240.1
	13:50	2.3	36.7	3.8	43.6	40.5	43.9	216.1
	18:00	2.5	40.3	3.7	52.4	46.4	48.6	410.6
	18:20	8.2	98.9	5.0	46.6	37.5	42.9	628.7
		30.6	**439.1**	**4.0**				**2,004.9**

4.2. Electrical demand simulations

Fig. 10 shows measured data for the multi-day experimental simulations performed for the PV subsystem with the selected PWM (Fig. 10a) and MPPT (Fig. 10b) charge controllers. The measured average simulated instensity on the two testing days was $696 \pm 30\,\mathrm{W/m^2}$, and $705 \pm 28\,\mathrm{W/m^2}$ for the PV subsystem with PWM and MPPT charge controller, respectively. The corresponding measured intensities on the lowest illuminated PV cells were $644\,\mathrm{W/m^2}$ and $655\,\mathrm{W/m^2}$, respectively. Laboratory ambient air temperature varied in the range ~20-27°C in both experimental simulations. Both PV subsystems supported the electrical load for a period of 24 hours on Day 1. On Day 2, the PWM charge controller disconnected the load at 20:21 h during the period of evening peak demand. However, the MPPT charge controller disconnected the electric load at 05:14 h towards the start of the next morning peak. The ability of the MPPT charge controller to operate the PV module at a higher voltage (i.e., 14.5-17.0 V) compared to the battery and load voltages is noticeable (see Fig. 10b) during the 6 h exposure period on both days. Table 8 compares the performance of the PV subsystem for both charge controllers. The current flow from the PV module in the MPPT case was lower than in the PWM case in correspondence to ohm's law. Experimental data shows that PV current with the PWM charge controller is 17.8% higher than that with the MPPT controller on Day 1 and 5% higher on Day 2. While this is of benefit for reduced cable losses and higher PV module efficiency, electricity yield improvement depends on the battery state of charge [59].

The PV energy yield, E_{PV} and PV module efficiency, η_{PV} were higher for the case of PWM charge controller when starting with a fully charged battery on Day 1 but higher for the case of MPPT charge controller on Day 2. Overall, the PV subsystem with an MPPT charge controller yielded higher energy and higher PV efficiency. The total energy supplied to the load was 9.2% greater for the PV subsystem with MPPT (as compared to the PWM), partly because the MPPT controller allowed the battery to reach a load disconnect voltage of 10.7 V, whereas the PWM controller instigated a disconnect voltage of 11.7 V. The MPPT charge controller could be a good alternative in the formulated AFRICaS PHST prototype, only if the related energy yield improvement relative to the PWM charge controller is sufficient to justify its unit cost. Further work is required to enhance this experimental methodology and derive an accurate energy balance for understanding system-wide energy flows for the PV subsystem.

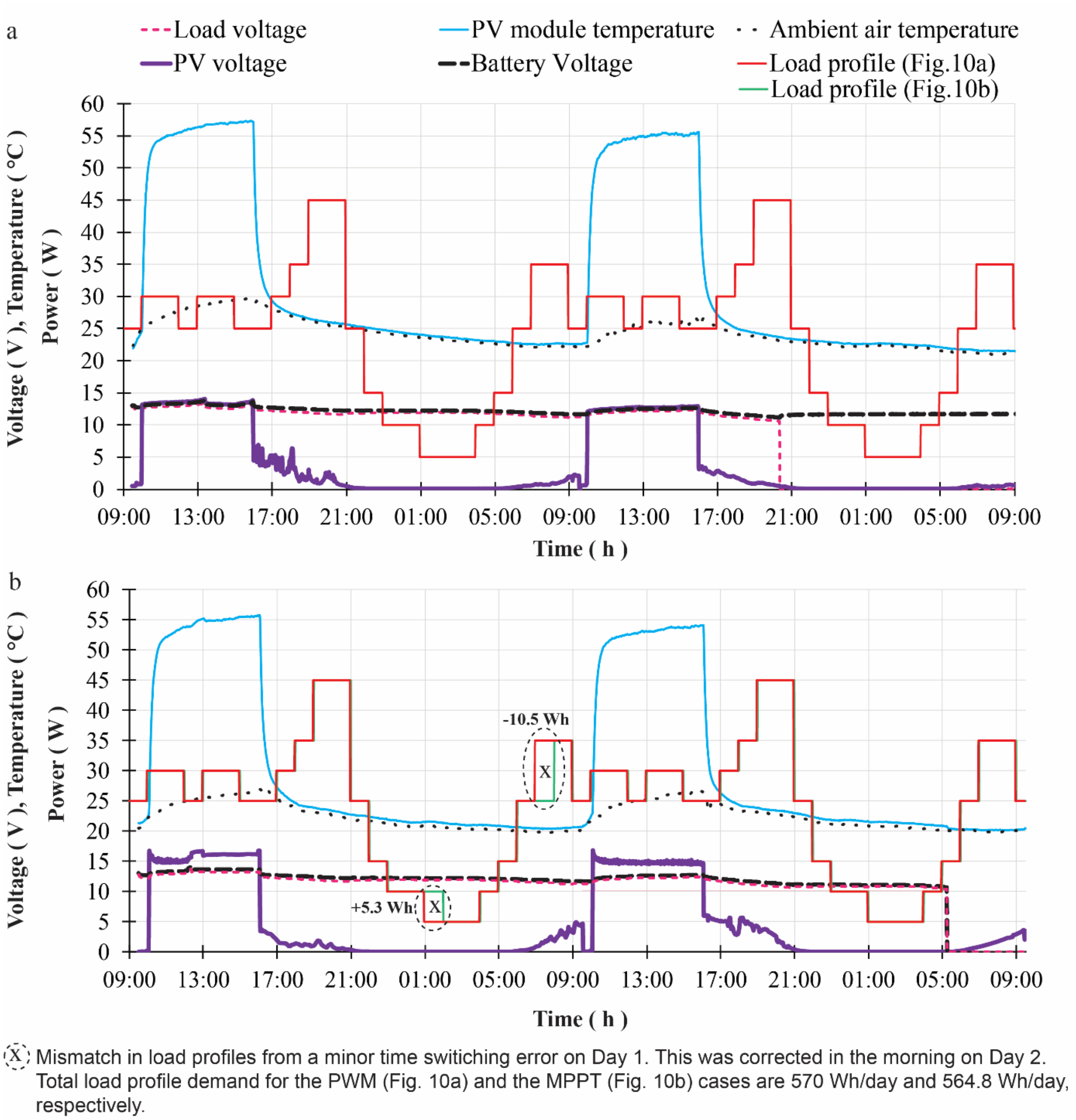

Fig. 10. Voltages (PV module, battery, and load), load profile power, ambient temperature, and PV cell temperature on two consecutive testing days for the (a) PWM charge controller and (b) MPPT charge controller cases.

Table 8

Comparisons of the performance of the PV subsystem with a PWM charge controller and MPPT charge controller.

Performance parameters	Unit	PWM charge controller			MPPT charge controller		
		DAY1	DAY2	**Total PWM**	DAY1	DAY2	**Total MPPT**
Minimum irradiance measured on PV module surface (G_{min})	W/m^2	644			655		
Energy supply from solar simulator for the 6 h exposure period ($E_{Sim \rightarrow PV}$)	Wh	2,256.8	2,256.8	**4,513.6**	2,295.4	2,295.4	**4,590.7**
PV energy yield (E_{PV})	Wh	280.6	265.5	**546.0**	269.2	295.9	**565.2**
Estimated efficiency of PV module (η_{PV})	%	12.4	11.8	**12.1**	11.7	12.9	**12.3**
Average PV module temperature during the 6 h exposure period	°C	55.3	53.7	-	53.0	51.7	-
Maximum PV module temperature	°C	57.4	55.6	-	55.8	54.1	-
Average laboratory ambient air temperature during the 6 h exposure period	°C	29.7	26.5	-	26.5	26.8	-
PV maximum power	W	48.4	45.2	-	56.2	55.9	-
Average PV supply current	A	3.48	3.50	-	2.86	3.33	-
PV maximum voltage	V	14.0	12.9	-	16.8	16.8	-
Battery maximum voltage	V	13.8	12.7	-	14.1	12.8	-
Battery minimum voltage	V	11.6	11.2	-	11.7	10.7	-
Energy supplied to load	Wh	668.2	352.5	**1,020.8**	654.4	470.0	**1,124.4**
Implemented load profile	Wh	570.0	570.0	**1,140.0**	564.8	570.0	**1,134.8**

5. Conclusion

This study develops an experimental methodology to evaluate a proposed Asymmetric Formed Reflector with Integrated Collector and Storage (AFRICaS) Partially Hybridised Solar Technology (PHST) prototype targeting the hot water and electricity demands of rural Sub-Saharan Africa households. The thermal energy output of the AFRICaS ICSSWH subsystem was $2{,}073.7 \pm 75.1$ kJ per day when supporting a daily hot water demand of 28 L, typical for a rural off-grid 4-person household in Sub-Saharan Africa. The solar thermal conversion efficiency for the different hot water draw-off experiments ranged from 28.0% to 30.6% with an average value of $29.4 \pm 1.0\%$. On average, the PV subsystem electrical yield and PV module efficiency was 273 Wh/day at 12.1% and 283 Wh/day at 12.3%, with the PWM and MPPT charge controller, respectively. The study found that in general a single AFRICaS ICSSWH prototype can deliver hot water at a consistent temperature during the day and satisfy the electrical energy demand of a typical rural household. The methodology has important future implications to test standards for guiding laboratory-based evaluation of Solar Home Systems (SHSs) for electricity and domestic hot water. While the results provide a better understanding of the likely performance of the presented AFRICaS PHST prototype, the method could be extended with appropriate instrumentation to enable an accurate determination of system-wide energy flows and energy balance. The thermal and electrical energy yields derived from the tests on the AFRICaS PHST prototype are valuable baselines for performing future techno-economic predictions to support the case for potential commercial deployment in off-grid Sub-Saharan African households. Further research may improve the current test methodology as regards measuring and ensuring a consistent initial battery charge state so that comparison tests can be undertaken fairly.

Declaration of Competing Interest

The authors declare that they have no known competing financial interests or personal relationships that could have appeared to influence the work reported in this paper.

Acknowledgements

The early stages of this work were financially supported through an International Studentship provided by the Department for Education (DfE), Northern Ireland, UK. Research proceeded with funding support from SolaForm Ltd and was completed as part of the "SwanaSmartStore" project funded by Innovate UK Energy Catalyst Round 7 (133910).

References

[1] United Nations. Transforming our world: The 2030 agenda for sustainable development (UNGA Resolution). New York: 2015.

[2] REN21. Renewables 2017 Global Status Report. Paris: REN21 Secretariat; 2017. https://doi.org/978-3-9818107-6-9.

[3] Muhumuza R. Solar cogeneration for access to energy in off-grid rural households in developing countries (DCs). Ulster Univerisy, UK, 2020.

[4] Besheer AH, Smyth M, Zacharopoulos A, Mondol J, Pugsley A. Review on recent approaches for hybrid PV/T solar technology. Int J Energy Res 2016;40:2038–53. https://doi.org/10.1002/er.3567.

[5] Lamnatou C, Chemisana D. Photovoltaic/thermal (PVT) systems: A review with emphasis on environmental issues. Renew Energy 2017;105:270–87. https://doi.org/10.1016/j.renene.2016.12.009.

[6] Jia Y, Alva G, Fang G. Development and applications of photovoltaic–thermal systems: A review. Renew Sustain Energy Rev 2019;102:249–65. https://doi.org/10.1016/j.rser.2018.12.030.

[7] Pang W, Cui Y, Zhang Q, Wilson GJ, Yan H. A comparative analysis on performances of flat plate photovoltaic/thermal collectors in view of operating media, structural designs, and climate conditions. Renew Sustain Energy Rev 2020;119:109599. https://doi.org/10.1016/j.rser.2019.109599.

[8] Kumar R, Rosen MA. A critical review of photovoltaic-thermal solar collectors for air heating. Appl Energy 2011;88:3603–14. https://doi.org/10.1016/j.apenergy.2011.04.044.

[9] Zondag HA. Flat-plate PV-Thermal collectors and systems: A review. Renew Sustain Energy Rev 2008;12:891–959. https://doi.org/10.1016/j.rser.2005.12.012.

[10] Mas'ud AA, Wirba AV, Muhammad-Sukki F, Albarracín R, Abu-Bakar SH, Munir AB, et al. A review on the recent progress made on solar photovoltaic in selected countries of sub-Saharan Africa. Renew Sustain Energy Rev 2016;62:441–52. https://doi.org/10.1016/j.rser.2016.04.055.

[11] Amanlou Y, Hashjin TT, Ghobadian B, Najafi G, Mamat R. A comprehensive review of Uniform Solar Illumination at Low Concentration Photovoltaic (LCPV) Systems. Renew Sustain Energy Rev 2016;60:1430–41. https://doi.org/10.1016/j.rser.2016.03.032.

[12] Cappelletti A, Reatti A, Martelli F. Numerical and experimental analysis of a CPV/T receiver suitable for low solar concentration factors. Energy Procedia 2015;82:724–9. https://doi.org/10.1016/j.egypro.2015.11.798.

[13] Sharaf OZ, Orhann MF. Concentrated photovoltaic thermal (CPVT) solar collector systems: Part II - Implemented systems, performance assessment, and future directions. Renew Sustain Energy Rev 2015;50:1566–633. https://doi.org/10.1016/j.rser.2014.07.215.

[14] Fuqiang W, Ziming C, Jianyu T, Yuan Y, Yong S, Linhua L. Progress in concentrated

solar power technology with parabolic trough collector system: A comprehensive review. Renew Sustain Energy Rev 2017;79:1314–28. https://doi.org/10.1016/j.rser.2017.05.174.

[15] Bhatia M, Angelou N. Beyond Connections Energy Access Redefined. World Bank. Energy Sector Management Assistance Program (ESMAP). Washington: 2015. https://doi.org/10.1596/24368.

[16] Muhumuza R, Zacharopoulos A, Mondol JD, Smyth M, Pugsley A. Energy consumption levels and technical approaches for supporting development of alternative energy technologies for rural sectors of developing countries. Renew Sustain Energy Rev 2018;97:90–102. https://doi.org/10.1016/j.rser.2018.08.021.

[17] Narayan N, Chamseddine A, Vega-Garita V, Qin Z, Popovic-Gerber J, Bauer P, et al. Exploring the boundaries of Solar Home Sysork for household electricity accesstems (SHS) for off-grid electrification: Optimal SHS sizing for the multi-tier framew. Appl Energy 2019;240:907–17. https://doi.org/10.1016/j.apenergy.2019.02.053.

[18] Keane J. Pico-solar Electric Systems, The Earthscan Expert Guide to the Technology and Emerging Market. 1st ed. Oxon: Routledge; 2014. https://doi.org/10.4324/9781315818467.

[19] Ayeng'o SP, Schirmer T, Kairies KP, Axelsen H, Uwe Sauer D. Comparison of off-grid power supply systems using lead-acid and lithium-ion batteries. Sol Energy 2018;162:140–52. https://doi.org/10.1016/j.solener.2017.12.049.

[20] Meyer JP. A review of domestic hot-water consumption in South Africa. R&D J 2000;16:55–61.

[21] Prinsloo GJ. Scoping exercise to determine load profile archetype reference shapes for solar co-generation models in isolated off-grid rural African villages. J Energy South Africa 2016;27:11–27. https://doi.org/10.17159/2413-3051/2016/v27i3a1375.

[22] Papakostas KT, Papageorgiou NE, Sotiropoulos BA. Residential hot water use patterns in Greece. Sol Energy 1995;54:369–74.

[23] Morante F, Zilles R. Energy demand in solar home systems: The case of the communities in Ribeira Valley in the State of São Paulo, Brazil. Prog Photovoltaics Res Appl 2001;9:379–88. https://doi.org/10.1002/pip.382.

[24] Kalogirou SA. Use of TRNSYS for modelling and simulation of a hybrid pv–thermal solar system for Cyprus. Renewabel Energy 2001;23:247–60. https://doi.org/10.1016/j.renene.2005.12.002.

[25] AEE INTEC. Thermal use of solar energy. Training course for experts and professionals. Southerm African Solar Thermal Training and Demonstration Initiative (SOLTRAIN). Feldgasse, Austria: 2009.

[26] Walker A. Solar Water Heating. Sol. energy Technol. Proj. Deliv. Build., New Jersey: John Wiley & Sons; 2013, p. 128–99.

[27] O'Sullivan K, Barnes D. Energy Policies and Multitopic Household Surveys: Guidelines for Questionnaire Design in Living Standards Measurement Studies. Washington, DC: 2007.

[28] AfDB. Green Mini-Grids in Sub-Saharan Africa: Analysis of barriers to growth and the potential role of the African Development Bank in supporting the sector. 2016.

[29] Smyth M, Eames PC, Norton B. Integrated collector storage solar water heaters. Renew Sustain Energy Rev 2006;10:503–38. https://doi.org/https://doi.org/10.1016/j.rser.2004.11.001.

[30] Singh R, Lazarus IJ, Souliotis M. Recent developments in integrated collector storage (ICS) solar water heaters: A review. Renew Sustain Energy Rev 2016;54:270–98. https://doi.org/https://doi.org/10.1016/j.rser.2015.10.006.

[31] Kumar R, Rosen MA. Solar Water Heaters with Integrated Collector-Storage Units. In: Harris AM, editor. Clean Energy Resour. Prod. Dev., Hauppauge, New York: Nova Science Publishers; 2011, p. 41–86.

[32] Pugsley A, Zacharopoulos A, Smyth M, Mclarnon D, Mondol J. SolaFin2Go field trials in Sub-Saharan Africa: Off-grid village electrification and hot water supply Needs analysis. 15th Photovolt. Sci. Appl. Technol. Conf., Coventry,UK: University of Warwick; 2019.

[33] Pugsley A. SolaFin2Go and SolaNetwork projects summary poster. Oppor. Energy Access SuperSolar Supergen Low Carbon Energy Dev. Netw. (LCEDN), 9th May 2019, Loughboroug, United Kingdom: Loughborough University; 2019, p. 1.

[34] Muhumuza R, Zacharopoulos A, Mondol JD, Smyth M, Pugsley A, Giuzio GF, et al. Experimental investigation of horizontally operating thermal diode solar water heaters with differing absorber materials under simulated conditions. Renew Energy 2019;138:1051–64. https://doi.org/10.1016/j.renene.2019.02.036.

[35] Hoffman LA, Ngo TT. Affordable solar thermal water heating solution for rural Dominican Republic. Renew Energy 2018;115:1220–30. https://doi.org/10.1016/j.renene.2017.09.046.

[36] Souliotis M, Papaefthimiou S, Caouris YG, Zacharopoulos A, Quinlan P, Smyth M. Integrated collector storage solar water heater under partial vacuum. Energy 2017;139:991–1002. https://doi.org/https://doi.org/10.1016/j.energy.2017.08.074.

[37] Arnaoutakis N, Souliotis M, Papaefthimiou S. Comparative experimental Life Cycle Assessment of two commercial solar thermal devices for domestic applications. Renew Energy 2017;111:187–200. https://doi.org/10.1016/j.renene.2017.04.008.

[38] Helal O, Chaouachi B, Gabsi S. Design and thermal performance of an ICS solar water heater based on three parabolic sections. Sol Energy 2011;85:2421–32. https://doi.org/10.1016/j.solener.2011.06.021.

[39] Mettawee EBS, Assassa GMR. Experimental study of a compact PCM solar collector. Energy 2006;31:2622–32. https://doi.org/10.1016/j.energy.2005.11.019.

[40] Varghese J, Samsher, Manjunath K. Techno-economic analysis of an integrated collector storage solar water heater with CPC reflector for households. Int J Ambient Energy 2018;39:885–90. https://doi.org/10.1080/01430750.2017.1354327.

[41] Smyth M, Barone G, Buonomano A, Forzano C, Giuzio GF, Palombo A, et al. Modelling and experimental evaluation of an innovative Integrated Collector Storage Solar Water

Heating (ICSSWH) prototype. Renew Energy 2020;157:974–86. https://doi.org/10.1016/j.renene.2020.05.074.

[42] Smyth M, Mondol JD, Muhumuza R, Pugsley A, Zacharopoulos A, McLarnon D, et al. Experimental characterisation of different hermetically sealed horizontal, cylindrical double vessel Integrated Collector Storage Solar Water Heating (ICSSWH) prototypes. Sol Energy 2020;206:695–707. https://doi.org/10.1016/j.solener.2020.06.056.

[43] Doorsamy W, Cronje WA. Sustainability of decentralized renewable energy systems in Sub-Saharan Africa. 2015 Int Conf Renew Energy Res Appl ICRERA 2015 2015;5:644–8. https://doi.org/10.1109/ICRERA.2015.7418491.

[44] Muhumuza R, Zacharopoulos A, Mondol JD, Smyth M, Pugsley A. Experimental study of heat retention performance of thermal diode Integrated Collector Storage Solar Water Heater (ICSSWH) configurations. Sustain Energy Technol Assessments 2019;34:214–9. https://doi.org/10.1016/j.seta.2019.05.010.

[45] Muhumuza R, Zacharopoulos A, Mondol JD, Smyth M, Pugsley A, McGee J. Simulation and experimental validation of solar radiation distribution on the absorber of a line-axis asymmetric compound parabolic concentrator. Sol Energy 2020;198:36–52. https://doi.org/10.1016/j.solener.2020.01.033.

[46] Smyth M, Quinlan P, Mondol JD, Zacharopoulos A, McLarnon D, Pugsley A. The evolutionary thermal performance and development of a novel thermal diode pre-heat solar water heater under simulated heat flux conditions. Renew Energy 2017;113:1160–7. https://doi.org/https://doi.org/10.1016/j.renene.2017.06.080.

[47] Smyth M, Quinlan P, Mondol JD, Zacharopoulos A, McLarnon D, Pugsley A. The experimental evaluation and improvements of a novel thermal diode pre-heat solar water heater under simulated solar conditions. Renew Energy 2018;121:116–22. https://doi.org/https://doi.org/10.1016/j.renene.2017.12.083.

[48] Pugsley A, Zacharopoulos A, Mondol JD, Smyth M. Theoretical and experimental analysis of a horizontal planar Liquid-Vapour Thermal Diode (PLVTD). Int J Heat Mass Transf 2019;144:118660. https://doi.org/10.1016/j.ijheatmasstransfer.2019.118660.

[49] NASA. NASA Prediction Of Worldwide Energy Resources, POWER Project Data Sets 2019. https://power.larc.nasa.gov/data-access-viewer/.

[50] Lorenzo E. Energy collected and delivered by PV modules. In: Luque A, Hegedus S, editors. Handb. Photovolt. Sci. Eng. 2nd ed., Chichester, West Sussex: Wiley; 2011, p. 905–70.

[51] Duffie JA, Beckman WA. Solar engineering of thermal processes. 4th ed. New Jersey: John Wiley & Sons; 2013.

[52] Wenham SR. Applied photovoltaics. Third. London: Earthscan; 2012.

[53] Daus Y, Kharchenko V, Yudaev IV. Solar radiation intensity data as basis for predicting functioning modes of solar power plants. In: Kharchenko V, Vasant P, editors. Handb. Res. Renew. Energy Electr. Resour. Sustain. Rural Dev., Harshey PA, USA: IGI Global; 2018, p. 283–309. https://doi.org/10.4018/978-1-5225-3867-7.ch012.

[54] Labouret A, Villoz M. Stand-alone photovoltaic generators. IET Renew. Energy Ser. 9

(English Transl. Sol. Photovolt. Energy, London: Institution of Engineering and Technology; 2010, p. 268–74.

[55] Nafeh AE-SA. Design and Economic Analysis of a Stand-Alone PV System to Electrify a Remote Area Household in Egypt. Open Renew Energy J 2009;2:33–7. https://doi.org/10.2174/1876387100902010033.

[56] Pode R. Financing LED solar home systems in developing countries. Renew Sustain Energy Rev 2013;25:596–629. https://doi.org/10.1016/j.rser.2013.04.004.

[57] Zacharopoulos A, Mondol JD, Smyth M, Hyde T, O'Brien V. State-of-the-art solar simulator with dimming control and flexible mounting. Proc. ISES Sol. World Congr. 2009 Renew. Energy Shap. Our Futur. 11-14 Oct., Johannesburg, South Africa: International Solar Energy Society; 2009, p. 854.

[58] EN ISO 9806:2017. Solar energy. solar thermal collectors. Test methods. 2018.

[59] Victron Energy. Which solar charge controller: PWM or MPPT? 2014. https://www.victronenergy.com/blog/2014/07/21/which-solar-charge-controller-pwm-or-mppt/.